Makara Journal of Science

Volume 25
Issue 2 *June*

Article 1

6-30-2021

Ambient Noise-Based Mapping of Bedrock Morphology and Potential Fissure Zone in East Tanjung Karang, Bandar Lampung, Lampung, Indonesia

Vico Luthfi Ipmawan
Department of Physics, Faculty of Science, Institut Teknologi Sumatera, Bandar Lampung 35365, Indonesia, vico.luthfi@fi.itera.ac.id

Ikah Ning Prasetiowati Permanasari
Department of Physics, Faculty of Science, Institut Teknologi Sumatera, Bandar Lampung 35365, Indonesia

Cahli Suhendi
Department of Geophysics Engineering, Faculty of Production and Industry Technology, Institut Teknologi Sumatera, Bandar Lampung 35365, Indonesia

Makara Journal of Science, 25/2 (2021), 61–68
doi: 10.7454/mss.v25i2.1205

Ambient Noise-Based Mapping of Bedrock Morphology and Potential Fissure Zone in East Tanjung Karang, Bandar Lampung, Lampung, Indonesia

Vico Luthfi Ipmawan[1*], Ikah Ning Prasetiowati Permanasari[1], and Cahli Suhendi[2]

1. Department of Physics, Faculty of Science, Institut Teknologi Sumatera, Bandar Lampung 35365, Indonesia
2. Department of Geophysics Engineering, Faculty of Production and Industry Technology, Institut Teknologi Sumatera, Bandar Lampung 35365, Indonesia

E-mail: vico.luthfi@fi.itera.ac.id

Received April 20, 2020 | Accepted May 27, 2020

Abstract

As a business center and the most populous subdistrict, East Tanjung Karang in Bandar Lampung, Lampung, Indonesia, is considered an area with excessive groundwater exploitation. This activity can trigger ground fissures that can consequently cause damage to buildings and roads. In this study, microtremor recordings from 17 sites were collected and analyzed by using the horizontal to vertical spectral ratio and ellipticity curve method. Results showed that the ground profiles of shear wave velocity from 17 sites ranged from 143.5 m/s to 1752.46 m/s, and they could be used to determine sediment layer and its thickness based on the SNI 1726-2012 criteria. The thickness of the bedrock varied from 8.18 m to 117.18 m. Bedrock morphology was obtained by subtracting the sediment thickness from the altitude value. The bedrock morphology and slope were then used to construct a potential fissure map of the area between Y16 and Y17 and between Y26 and Y27, which had high bedrock slopes (more than 45°). The ground fissure potential in these areas was higher than that in other areas. Such areas also had a geological hazard potential from ground fissures caused by excessive groundwater exploitation. Our study could be used by authorities as a basis for preventing subsidence-related disasters in this subdistrict.

Keywords: ellipticity curve method, excessive groundwater exploitation, horizontal to vertical spectral ratio, microtremor

Introduction

Earth fissures (or simply fissures) are large cracks formed in the ground as a result of soil surface tension due to land subsidence (i.e., lowering of the ground surface elevation). Land subsidence is mainly caused by groundwater pumping. As the most populous district in Bandar Lampung, East Tanjung Karang has 18.280 inhabitants/ km^2 [1], and these inhabitants have a high demand for clean water (± 135 L/inhabitant/day). However, only 65% of this demand can be served by Perusahaan Dagang Air Minum (a government water company) Way Rilau [2]. As such, inhabitants fulfill this deficiency through groundwater self-exploitation. Hotels and business centers in East Tanjung Karang also have their groundwater drilling wells. Consequently, excessive groundwater exploitation can cause land subsidence and fissure.

Microtremor data have been widely used not only for determining a particular effect on sites but also for identifying zones of potential fissure. Information about these zones can be obtained on the basis of fundamental frequency (*fo*), shear wave velocity (*Vs*), sediment thickness, and altitude of a site. Horizontal to vertical spectral ratio (HVSR) is a basic method commonly used to assess *fo* [3–4]. *Vs* can be acquired by geotechnical sounding [4] or spatial autocorrelation [3]. The thickness of a sediment can be calculated from equations involving *Vs* and *fo*. In Mexico, microtremor measurement is conducted to infer the potential of fissures and cracks in a specific basin. Cracking and fissuring occur when the gradient in the depth of the hard layer below the soft clay is sharp [4]. Bedrock mapping can be improved via an interpolation approach that involves geostatistical analysis with resonance frequency [5].

Earth fissure can cause various damages, such as cracked roads, pipeline breakage, and collapsed buildings. A potential fissure zone should be mapped to provide the society and the government with information about the negative impacts of fissuring due to excessive groundwater extraction. Mapping also helps yield information for planning groundwater utilization in Bandar Lampung, a subdistrict in East Tanjung Karang.

In this study, ambient noise recordings or microtremors from 17 sites in the East Tanjung Karang subdistrict were analyzed using the HVSR method. An HVSR curve was obtained and used as input for the ellipticity curve method. A ground profile of *Vs* was determined to assess the thickness of sediment layers, and bedrock morphology was examined by subtracting sediment thickness from altitude. The slope was determined on the basis of the contour of the bedrock, and a map showing the potential fissure zone was created.

Methods

On July 7–9, 2019, microtremor data from 17 locations in East Tanjung Karang were recorded using a C100 GEObit seismometer, which is a short-period type with sampling at 100 Hz frequency. The average duration of the recordings per location was 60 min. The study area is located at 105.2608° E to 105.2746° E and 5.41869° S to 5.40368° S.

HVSR, introduced by Nakamura [6], is used to assess *fo* and amplification responses that describe the nature of a local site. This method is commonly utilized to evaluate some characteristics of soft sedimentary (soil) deposits [7–8]. It has been frequently adopted in seismic vulnerability and microzonation investigations because of its low cost for survey and analysis [9]. Some assumptions were presented by Nakamura [6]. First, Rayleigh wave is a noise that affects the sediment layer surface only. Second, a sediment layer does not amplify ambient noise spectra in a vertical channel. Third, Rayleigh wave has the same effect on vertical and horizontal channels. Fourth, vertical and horizontal ambient noise spectra have the same value in a bedrock layer. HVSR can be expressed as follows:

$$HVSR = T_{site} = \frac{S_{HS}}{S_{VS}} = \frac{\sqrt{\left[\left(S_{NS}\right)^2 + \left(S_{EW}\right)^2\right]}}{S_V}, \quad (1)$$

where S_{HS} is the horizontal ambient noise spectrum on the surface, S_{VS} is the vertical ambient noise spectrum on the surface, S_{NS} is the recorded horizontal ambient noise spectrum in the north–south direction, S_{EW} is the recorded horizontal ambient noise spectrum in the east–west direction, and S_V is the recorded vertical ambient noise spectrum.

A three-component seismometer was deployed for approximately 1 h to obtain microtremor data from 17 locations at East Tanjung Karang, Bandar Lampung, Lampung, Indonesia. The microtremor data were processed with the open software Geopsy for drawing HVSR curves. Some transient signals were first removed automatically with the short-term average/long-time average (STA/LTA) method and then removed manually to improve the quality of data. STA and LTA were set at 1 and 30 s, respectively. The minimum and maximum STA/LTA were set at 0.2 and 2 s, respectively. If some long transient data were chosen after the STA/LTA method was applied, then they were removed manually. Long transient data appeared because of a heavy human activity or traffic, and they were eliminated to keep the most stationary parts of microtremor data. Free-transient microtremor data were subjected to fast Fourier transform and Konno–Ohmachi smoothing. The result was an HVSR curve from which the dominant frequency was obtained. However, the criteria of reliability must be fulfilled before the dominant frequency was determined. In the SESAME project [9], a process for evaluating the reliability of the HVSR curve was outlined in accordance with the following criteria: (i) for the peak to be significant, *fo* should be >10 divided by the window length (Iw); (ii) the number of significant cycles should be >200; and (iii) the standard deviations of the amplitude of the HVSR curve at frequencies between 0.5*fo* and 2*fo* should be <2 and <3 when *fo* is >0.5 Hz and <0.5 Hz, respectively. All these criteria must be satisfied for a curve to be considered reliable and useful for further analysis.

The ellipticity curve method is an inverse modeling used for determining a ground profile based on wave velocity. In this method, an HVSR curve is used as input, but it is affected by some parameters, such as Poisson's ratio, *Vs*, compression wave velocity (*Vp*), and density.

The ground profile of *Vs* having the lowest misfit is utilized as a basis for interpreting sediment layers. The misfit is calculated with the following equation [10]:

$$misfit = \sqrt{\frac{1}{N}\sum_{i=1}^{N}\left(\frac{D_i - M_i}{\sigma_i}\right)^2}, \quad (2)$$

where N is the point data, Di is the inversion data, Mi is a ground structure model, and σ, is the standard deviation of inversion data. Ellipticity curve modeling was run in Dinver, open-source software for surface wave inversions. The ground profile of *Vs* for each site point was obtained. The input of the modeling was the HVSR curve obtained from Geopsy. *Vp*, Poisson's ratio, *Vs*, and density were filled as the parameter constraints in the modeling. *Vp* ranged from 200 m/s to 5000 m/s, whereas *Vs* ranged from 150 m/s to 3500 m/s. The assumption that *Vp* > *Vs* was selected in the Diver program in accordance with elastic seismic wave theory. Poisson's ratio and density varied from 0.05 to 0.4 and from 1500 kg/m^3 to 5000 kg/m^3, respectively, based on the lithology of East Tanjung Karang, that is, andesitic–basaltic lava, breccia, and tuff [11]. The six-layer ground model was chosen on the basis of the results of a research on multichannel analysis surface waves in Tanjung Karang [12].

After *Vs* and *fo* were acquired via the ellipticity and HVSR method, respectively, the thickness of sediment layers could be obtained using the following equation [3]:

$$H = \frac{V_s}{4 f_o} . \quad (3)$$

Results and Discussion

The output of the HVSR method is the HVSR curve, and *fo* can be read directly from the curve. The dominant frequency ranges from 0.61 Hz to 1.13 Hz. Figure 1 depicts some HVSR curves in East Tanjung Karang, and Table 1 presents all the dominant frequencies.

In Table 1, all the dominant frequencies in this study were less than 2.5 Hz, indicating that all the microtremor recording sites had a thick sediment layer (more than 30 m) according to Kanai's soil classification [13]. The area with a relatively high value was in the north of East Tanjung Karang, and the highest value was in Y18, which was in the south of East Tanjung Karang. The dominant frequency distribution is illustrated in Figure 2.

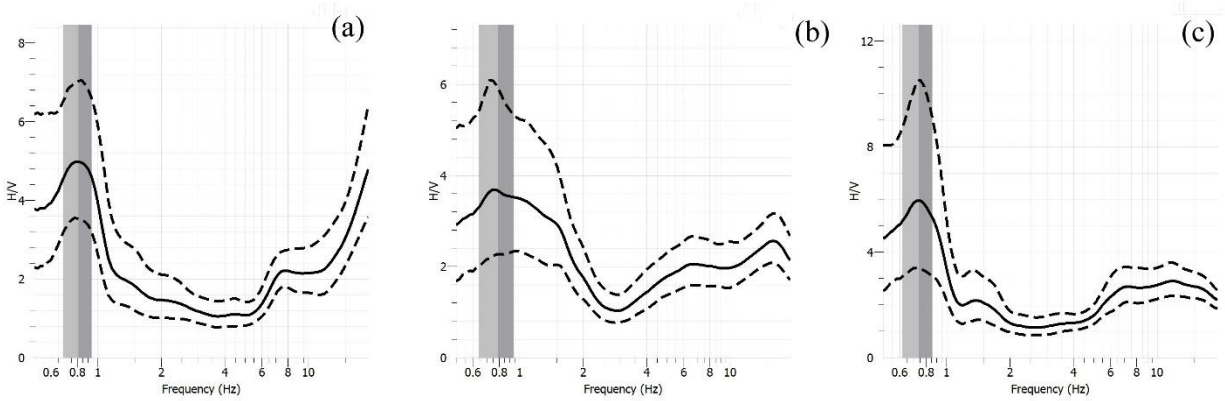

Figure 1. Some HVSR Curves in East Tanjung Karang. HVSR Curves in (a) Y6, (b) Y16, and (c) Y26. The Solid Line is the Average of the HVSR Curve of Each Window. The Upper Dashed Line is the Maximum Standard Deviation, and the Lower Dashed Line is the Minimum Standard Deviation of the HVSR Curve of all the Windows

Table 1. Dominant Frequency in Each Recording Site in East Tanjung Karang

Site Name	Longitude (°)	Latitude (°)	*fo* (Hz)
Y1	105.2608	−5.40368	0.92
Y2	105.2647	−5.40642	0.91
Y3	105.2677	−5.40648	1.07
Y4	105.2614	−5.41030	0.63
Y5	105.2647	−5.40924	0.68
Y6	105.2672	−5.40915	0.81
Y8	105.2652	−5.41268	0.66
Y9	105.2632	−5.41362	0.65
Y13	105.265	−5.41500	0.61
Y14	105.2684	−5.41625	0.69
Y15	105.2697	−5.41495	0.65
Y16	105.2732	−5.41439	0.83
Y17	105.2746	−5.41482	0.70
Y18	105.2673	−5.41870	1.13
Y22	105.2746	−5.41653	0.72
Y26	105.2727	−5.41876	0.73
Y27	105.2745	−5.41869	0.78

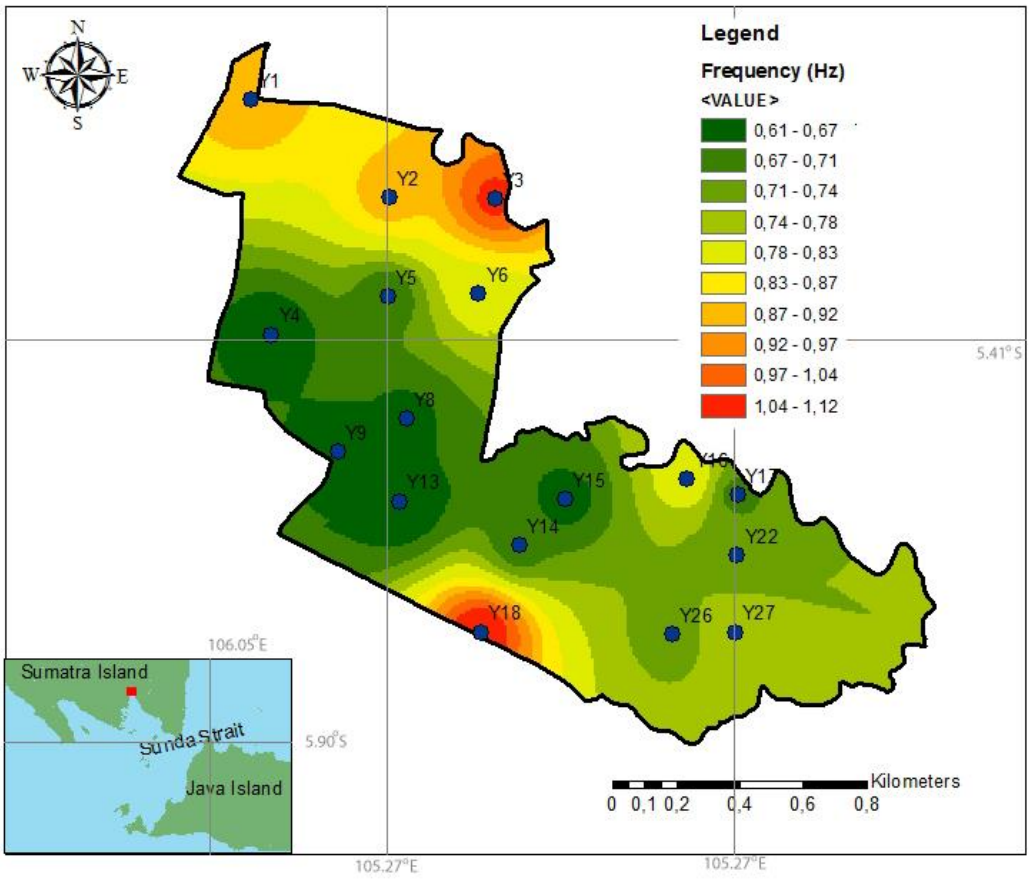

Figure 2. Dominant Frequency Distribution in East Tanjung Karang

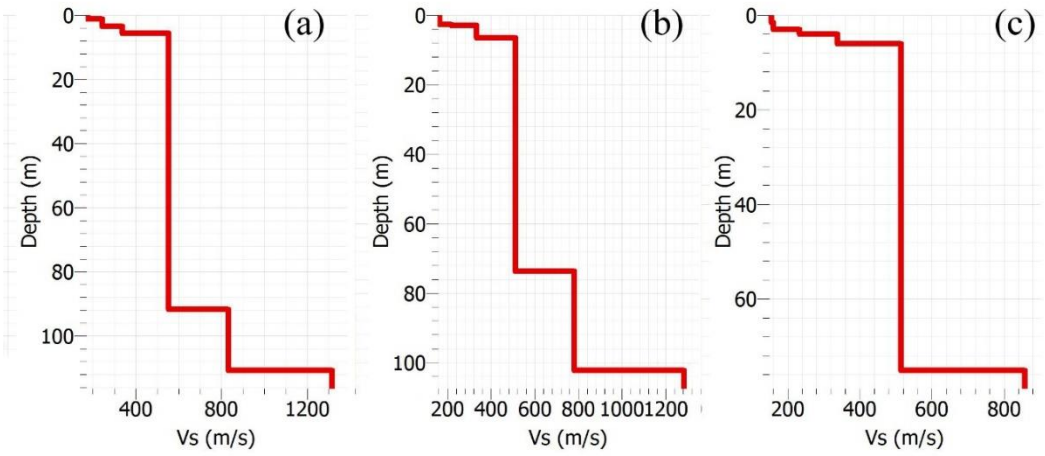

Figure 3. Ground Profiles from *Vs* Model. Ground Profiles of *Vs* in (a) Y6, (b) Y16, and (c) Y26

All the microtremor recording sites are found in areas with young volcanic deposits of Gunung Betung (Qhv-b) [11]. These deposits consist of andesitic–basaltic lava, breccias, and tuff. According to ellipticity curve modeling, *Vs* ranges from 143.5 m/s to 1752.46 m/s. Figure 3 shows some ground profiles of *Vs* model. Shear wave values can be used to classify sites based on the SNI 1726–2012 criteria (Table 2). *Vs* and class of the microtremor recording sites are listed in Table 3.

The sediment layer in this study was correlated with the site classification based on SNI 1726-2012. In particular,

soft soil (SE), medium hard soil (SD), and hard soil (SC) can be considered sediment layers. The thickness of sediment layers based on the assumption for each microtremor recording site is shown in Table 4. The thickness of the sediment ranges from 8.18 m to 117.8 m, and the average thickness of the sediment is 65.9 m.

The bedrock morphology in East Tanjung Karang is defined as a value obtained by subtracting sediment thickness from altitude. The results can be interpolated for each recording site to produce the contour of a bedrock.

Table 2. Soil Classification based on the SNI 1726-2012 Criteria Related to *Vs*

Site Class	*Vs* (m/s)
SA (hard rock)	>1500
SB (rock)	750–1500
SC (hard soil, very dense, and soft rock)	350–750
SD (medium hard soil)	175–350
SE (soft soil)	<175

Table 3. *Vs* and Class of Microtremor Recording Sites

Site Name	Layer	Initial Depth (m)	End Depth (m)	Shear wave velocity (m/s)	Site Class	Site Name	Layer	Initial Depth (m)	End Depth (m)	Shear wave velocity (m/s)	Site Class
Y1	1st	0	3.61	152.87	SE	Y13	1st	0	1.71	164.8	SE
	2nd	3.61	5.42	256.42	SD		2nd	1.71	3.76	238.47	SD
	3rd	5.42	15.81	411.74	SC		3rd	3.76	10.94	336.7	SD
	4th	15.81	42.45	651.19	SC		4th	10.94	18.8	410.37	SC
	5th	42.45	83.1	864.75	SB		5th	18.8	63.32	557.72	SC
	6th	83.1	86.26	987.71	SB		6th	63.32	65.28	950.63	SB
Y2	1st	0	2.2	205.09	SD	Y14	1st	0	2.02	164.4	SE
	2nd	2.2	3.31	268.51	SD		2nd	2.02	4.04	229.83	SD
	3rd	3.31	9.37	433.39	SC		3rd	4.04	6.06	360.68	SC
	4th	9.37	78.25	712.43	SC		4th	6.06	18.47	475.18	SC
	5th	78.25	101.4	1092.93	SB		5th	18.47	52.82	679.63	SC
	6th	101.4	105.8	1752.46	SA		6th	52.82	55.12	1227.58	SB
Y3	1st	0	1.27	143.5	SE	Y15	1st	0	2.51	164.41	SE
	2nd	1.27	3.8	156.59	SE		2nd	2.51	5.03	255.63	SD
	3rd	3.8	34.84	246.28	SD		3rd	5.03	6.11	367.13	SC
	4th	34.84	73.48	397.43	SC		4th	6.11	7.18	407.68	SC
	5th	73.48	117.18	572.76	SC		5th	7.18	66.1	519.17	SC
	6th	117.18	122.25	905.28	SB		6th	66.1	68.97	792.92	SB
Y4	1st	0	1.09	177.53	SD	Y16	1st	0	3.34	164.33	SE
	2nd	1.09	4.36	195.01	SD		2nd	3.34	3.91	233.18	SD
	3rd	4.36	7.64	334.85	SD		3rd	3.91	6.68	336.00	SD
	4th	7.64	52.92	463.04	SC		4th	6.68	74.02	516.71	SC
	5th	52.92	100.39	637.83	SC		5th	74.02	104.08	778.73	SB
	6th	100.39	105.3	894.2	SB		6th	104.08	106.3	1284.72	SB
Y5	1st	0	3.17	160.56	SE	Y17	1st	0	7.04	286.35	SD
	2nd	3.17	5.07	225.62	SD		2nd	7.04	8.32	440.34	SC
	3rd	5.07	32.3	342.73	SD		3rd	8.32	17.91	732.21	SC
	4th	32.3	97.55	420.79	SC		4th	17.91	71.01	841.88	SB
	5th	97.55	116.55	615.97	SC		5th	71.01	119.00	1161.02	SB
	6th	116.55	121.62	967.28	SB		6th	119.00	122.83	1728.37	SA

Table 3. *Continue*

Site Name	Layer	Initial Depth (m)	End Depth (m)	Shear wave velocity (m/s)	Site Class	Site Name	Layer	Initial Depth (m)	End Depth (m)	Shear wave velocity (m/s)	Site Class
Y6	1st	0	1.21	166.21	SE	Y18	1st	0	1.9	180.23	SD
	2nd	1.21	3.62	239.9	SD		2nd	1.9	5.07	263.18	SD
	3rd	3.62	6.09	350.43	SC		3rd	5.07	12.67	449.81	SC
	4th	6.09	91.67	553.08	SC		4th	12.67	65.88	646.81	SC
	5th	91.67	110.89	820.2	SB		5th	65.88	117.82	864.55	SB
	6th	110.89	115.72	1326.81	SB		6th	117.82	122.22	1476.29	SB
Y8	1st	0	2.16	182.93	SD	Y22	1st	0	3.27	190.45	SD
	2nd	2.16	3.03	210.14	SD		2nd	3.27	4.91	333.82	SD
	3rd	3.03	5.84	305.37	SD		3rd	4.91	6.00	432.38	SC
	4th	5.84	22.49	455.02	SC		4th	6.00	8.18	530.49	SC
	5th	22.49	40.23	652.28	SC		5th	8.18	94.85	817.66	SB
	6th	40.23	41.23	1067.2	SB		6th	94.85	104.21	1301.51	SB
Y9	1st	0	2.71	161.07	SE	Y26	1st	0	1.79	150.41	SE
	2nd	2.71	3.61	212.68	SD		2nd	1.79	3.14	162.43	SE
	3rd	3.61	4.52	277.19	SD		3rd	3.14	4.26	228.66	SD
	4th	4.52	14.00	393.31	SC		4th	4.26	6.05	331.96	SD
	5th	14.00	83.55	619.11	SC		5th	6.05	75.1	516.02	SC
	6th	83.55	86.26	986.26	SB		6th	75.1	78.91	858.06	SB
						Y27	1st	0	1.71	159.52	SE
							2nd	1.71	2.18	215.25	SD
							3rd	2.18	5.29	289.57	SD
							4th	5.29	9.66	394.85	SC
							5th	9.66	28.34	593.03	SC
							6th	28.34	30.06	946.01	SB

Table 4. *Vs* and Class of Each Microtremor Recording Site

Site Name	Sediment Thickness (m)	Altitude (masl)	Bedrock depth from surface (m)
Y1	42.45	101	58.55
Y2	78.25	101	22.75
Y3	117.18	100	−17.18
Y4	100.39	103	2.61
Y5	116.55	106	−10.55
Y6	91.67	96	4.33
Y8	40.23	106	65.77
Y9	83.55	110	26.45
Y13	63.32	100	36.68
Y14	52.82	93	40.18
Y15	66.10	99	32.9
Y16	74.02	95	20.98
Y17	17.91	100	82.09
Y18	65.88	99	33.12
Y22	8.18	97	88.82
Y26	75.10	83	7.900
Y27	28.34	98	69.66

A fissure-vulnerable zone is determined with bedrock slope. The higher the slope, the higher the fissure potential. The map of the slope of the bedrock is illustrated in Figure 4. The areas between Y16 and Y17 and between Y26 and Y27 have high slopes (more than 45°). Their ground fissure potential is also higher than that of other areas, and such areas are relatively susceptible to ground fissure caused by excessive water exploitation.

The study area is located in a site with distal deposit (±12 km away) from Gunung Betung as a source. As such, deposits are normally not too thick. However, the deposit in the study area is thick and can be obtained from single or multiple eruptions over a long period. Our findings suggest that the sediment layer in the study area is composed of tuff from young volcanic deposit formation (Qhv), whereas the bedrock layer is made of welded tuff from Lampung formation, an older formation (QTl). The compactness of welded tuff is higher than that of tuff.

The tuff exhibits porosities ranging from 30% to 40%, highlighting its potential as an aquifer. The geomechanical property of tuff is very weak, and its deformability is

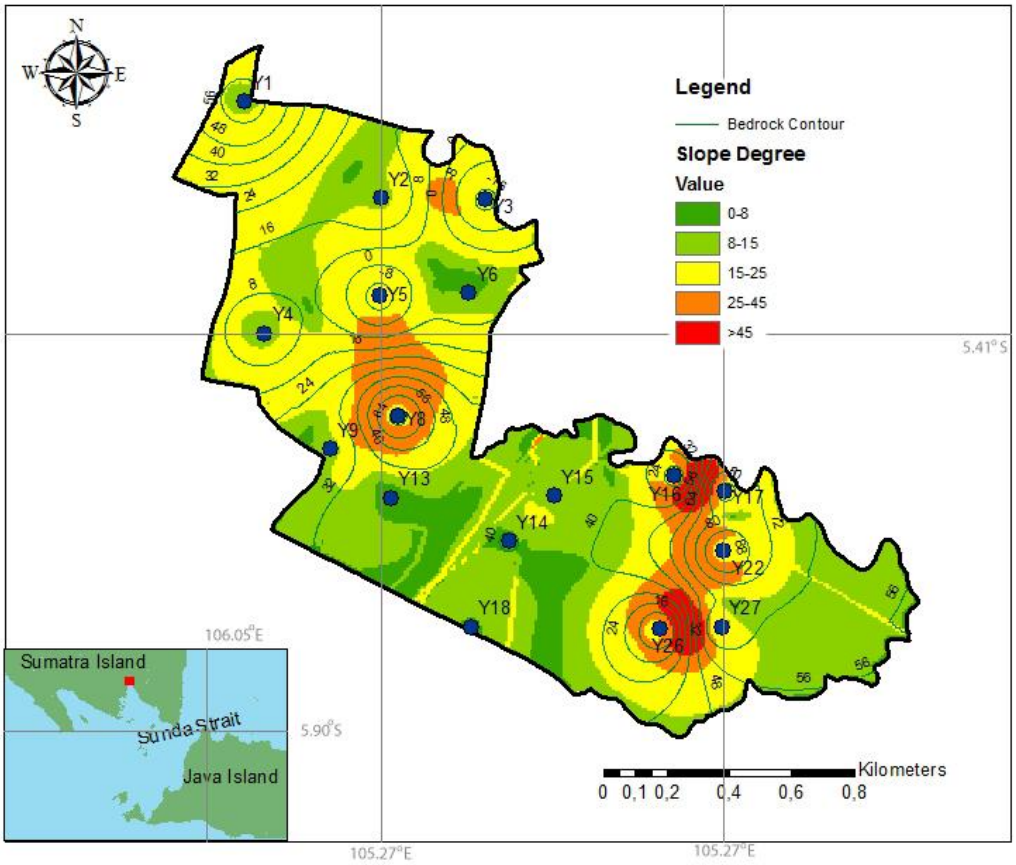

Figure 4. Bedrock Contour Map Over East Tanjung Karang. The Color Represents the Slope of the Bedrock

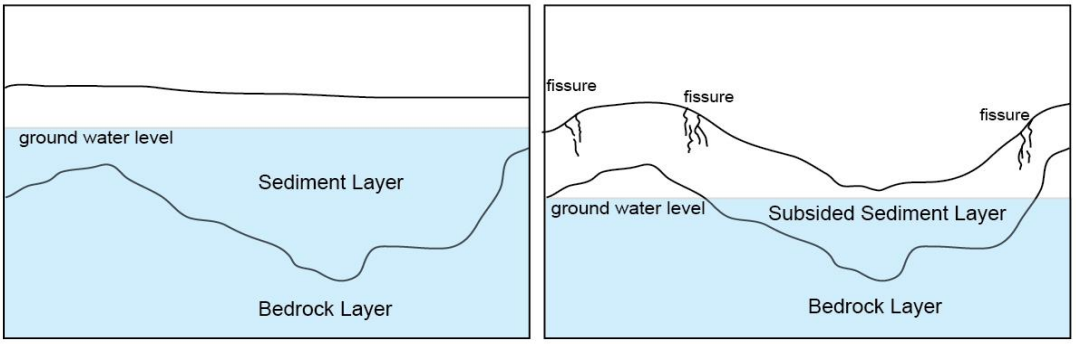

Figure 5. Illustration of Ground Subsidence (Modified from [4]). Before the Subsidence of Ground Water Surface in the Sediment Layer (left). After the Subsidence of Ground Water Surface in the Sediment Layer (right)

high [14]. If a water resource is overexploited, then land subsidence easily occurs because of these properties and the gravitation effect. The subsidence of the ground water surface in the sediment layer likely causes compaction, resulting in a ground subsidence. Otherwise, it unlikely occurs in the bedrock layer because it is composed of a hard rock type. Cracking and fissuring take place when the degree of the slope of the bedrock layer below the sediment layer is high. Ground subsidence is illustrated in Figure 5.

Conclusion

Microtremor investigations on 17 sites in East Tanjung Karang yielded the following conclusions: (a) The study area exhibited frequencies ranging from 0.61 Hz to 1.13 Hz, indicating that all microtremor recording sites had a thick sediment layer (more than 30 m); (b) The sampled areas produced *Vs* varying from 143.5 m/s to 1752.46 m/s; Frequency and velocity data were used to calculate sediment thickness that varied from 8.18 m to 117 m; (c) The mapping of bedrock morphology and slope was used to construct a potential fissure map of the area, specifically the area between Y16 (105.2732° E, −5.41439° S) and Y17 (105.2734° E, −5.41482° S) and between Y26 (105.2727° E, −5.41476° S) and Y27 (105.2745° E, −5.41869° S). Both areas had a high bedrock slope (more than 45°), and their ground fissure potential was higher than those in other areas. Such areas also had a geological hazard potential from ground fissures caused by excessive groundwater exploitation; (d) Our study could be useful for the local government that would conduct urban land use planning and authorities that would develop preventive measures against subsidence-related disasters in East Tanjung Karang.

Acknowledgements

The authors would like to thank Institut Teknologi Sumatera for providing the research grant (No. B/302/IT9.C1/PT.01.03/2019) through “Hibah Penelitian ITERA SMART 2019.”

References

[1] BPS Bandar Lampung. 2017. Kecamatan Tanjung Karang Timur dalam Angka 2017. https://bandarlampungkota.bps.go.id/publication/2017/09/20/3e074dbbc4eedd4934f11672/kecamatan-tanjungkarang-timur-dalam-angka-2017.html.

[2] Ditjen Cipta Karya. 2001. Profil Kabupaten/Kota: Kota Bandar Lampung. http://ciptakarya.pu.go.id/pr ofil/profil/barat/lampung/lampung.pdf.

[3] Prabowo, U.N., Marjiyono, Sismanto. 2016. Mapping the fissure potential zones based on microtremor measurement in Denpasar City, Bali. IOP Conf. Ser. Earth Environ. Sci. 29: 012012, https://doi:10.1088/1755-1315/29/1/012012.

[4] Shelley, E.O., Javier L.S., Gabriel A., Edgar M.S. 2012. Microtremor Measurements to Identify Zones of Potential Fissuring in The Basin of Mexico. J. Geofis. Int. 51(2): 143–156.

[5] Trevisani, S., Boaga, J., Agostini, L., Galgaro, A. 2017. Insights into bedrock surface morphology using low-cost passive seismic surveys and integrated geostatistical analysis. Sci. Total Environ. 578: 186–202, https://doi.org/10.1016/j.scitotenv.2016.11.04 1.

[6] Nakamura, Y. 1989. A method for dynamic characteristics estimation of subsurface using microtremor on the ground surface. Q. Rep. RTRI. 30: 25–33.

[7] Ipmawan, V.L., Permanasari, I.N.P., Siregar, R.N. 2019. Spatial Analysis of Seismic Hazard based on Dynamical Characteristics of Soil in Kota Baru, South Lampung. J. Sci. Appl. Technol. 2(1): 169–175, https://doi.org/10.35472/281437.

[8] Ipmawan, V., Permanasari, I., Siregar, R. 2019. Determining Soft Layer Thickness Using Ambient Seismic Noise Record Analysis in Kota Baru, South Lampung. Makara J. Sci. https://doi/org/10.745 4/mss.v23i1.10802.

[9] SESAME European Research Project. 2004. Guidelines for the implementation of the H/V spectral ratio technique on ambient vibrations measurements, processing and interpretation. ftp://ftp.geo.uib.no/pub/seismo/SOFTWARE/SESAME/USER-GUIDELINES/SESAME-HV-User-Guidelines.pdf.

[10] Burger, H.R. 1992. Exploration Geophysics of the Shallow Subsurface. Prentice Hall.

[11] Manggala, S.A., Amiruddin, T., Surwati, S., Gafoer, Sidarto. 1993. Geological Map of Tanjung Karang Quadrangle, Geological Research and Development Centre.

[12] Laksono, A., Rasimeng, S., Rustadi. 2019. Intepretasi nilai kecepatan gelombang geser (Vs 30) menggunakan metode seismik *multichannel analysis of surface wave (masw)* untuk memetakan daerah rawan gempa bumi di Kota Bandar Lampung. Jurnal Geofisika Eksplorasi. 3(3), (in Indonesian) http://dx.doi.org/10.23960/jge.v3i3.1044.

[13] Parolai, S., Bormann, P., Milkereit, C. 2001. Assessment of natural frequency of the sedimentary cver in the Cologne area (Germany) using noise measurement. J. Earthqu. Eng. 5: 541–564, https://doi.org/1 0.1080/13632460109350405.

[14] Aydan, O., Ulusay, R. in: Ulusay, R., Aydan, O., Gerçek, H., Hindistan, M., Tuncay, E. (eds.). 2016. Rock Mechanics and Rock Engineering: From the Past to the Future. CRC Press. pp. 829–835.